CLAS12 Run Group G Jeopardy Update Document

W.K. Brooks [a], H. Hakobyan, B. Kopeliovich,[1] K. Adhikari, S. Bültmann, S.E. Kuhn [b], V. Lagerquist, P. Pandey,[2] C.D. Keith, J.D. Maxwell,[3] K. Griffioen,[4] Raphaël Dupré,[5] N. Kalantarians,[6] D. Keller,[7] E. Long, K. Slifer, M. McClelland, L. Kurbany, T. Anderson, E. Mustafa, D. Ruth, N. Santiesteban,[8] C. Djalai,[9] A.W. Thomas,[10] E. Pace,[11] C. Ciofi, M. Rinaldi, S. Scopetta,[12] V. Guzey,[13] M. Strikman,[14] I. Cloët,[15] and W. Bentz[16]

[1] *Universidad Técnica Federico Santa María, Valparaíso, Chile*
[2] *Old Dominion University, Norfolk, VA 23529*
[3] *Jefferson Lab, Newport News, VA 23606*
[4] *College of William and Mary, Williamsburg, VA*
[5] *Université Paris-Saclay, CNRS, 911405 Orsay, France*
[6] *Virginia Union University, Richmond, VA*
[7] *University of Virginia, Charlottesville, VA*
[8] *University of New Hampshire, Durham, NH*
[9] *Ohio University, Athens, OH*
[10] *University of Adelaide, Australia*
[11] *University of Rome Tor Vergata, Italy*
[12] *University of Perugia, Italy*
[13] *Petersburg Nuclear Physics Institute, Russia*
[14] *Pennsylvania State University, PA*
[15] *Argonne National Laboratory, IL*
[16] *Tokai University, Japan*

(Dated: June 18, 2020)

We summarize the case for renewing the PAC approval for Run Group G with the full allocated beam time.

I. INTRODUCTION

Run Group G (RG-G) is the designation for a CLAS12 run period of 55 PAC days with polarized proton (^{6}LiH) and Lithium-7 (^{7}LiD) targets in an 11 GeV electron beam. This run period will collect data for Experiment E12-14-001 (S. Kuhn and W. Brooks [a], spokespersons), "The EMC Effect in Spin Structure Functions [1]." The experiment was approved for 55 PAC days (50 days of production running and 5 days of auxiliary runs) by PAC42 in 2014, with a scientific rating of B+.

The centerpiece of RG-G, the polarized target, is on track to be ready by summer 2021, and will be used for a first run of RG-C in Fall/Winter 2021/2022. The technique of polarizing 2 target cells simultaneously but with separate polarization has been demonstrated, and all required technical components for a successful run of RG-G are either in hand or have been fully prototyped.

II. PHYSICS GOALS

The long-standing puzzle of the origin of the EMC effect has received an increasing level of attention over the six years since Experiment E12-14-001 was initially proposed. Many new publications by the proponents of both leading models (EMC effect attributed to short-range correlations (SRC) in nuclei *vs.* mean-field nuclear binding) have appeared [2–8]. The EMC-SRC connection, proposed nearly a decade ago [9], was prominently highlighted in a recent Nature publication [2] where the case was strengthened by demonstrating the existence of a universal function describing the EMC effect for all nuclei, including deuterium. This universal function was based on the assumption that the EMC effect is entirely due to the nucleon structure modifications present in SRC interactions. This year, new and sophisticated calculations [7] have been performed to examine the assertion of a connection between the EMC effect and the phenomena associated with short range correlated nucleon pairs. These new calculations test the EMC-SRC connection for the deuteron using several models that individually succeed in describing DIS on nuclei. These models take into account nuclear binding, Fermi motion, and nucleon off-shell effects, and they allow the

[a] contact person
[b] spokesperson

contributions to structure function calculations to be classified into low momentum and high momentum components. They found that high-momentum nucleons, such as those found in SRCs, were not the main source of the EMC effect in the models they studied. Hence, it is highly desirable to measure new observables that are uniquely sensitive to the differences between these two explanations.

The scientific aim of E12-14-001 is to probe the spin dependence of the modifications of proton structure arising from the nuclear medium. Several theoretical models predict that such effects are substantial and different from the spin-averaged medium ("EMC") effect, although they differ from each other in some details, such as the role played by sea quarks. Many experimental measurements have been performed to quantify the modification of the quark structure of nucleons in the three decades since the original EMC papers were published, with substantial advances coming from Jefferson Lab experiments. However, no experiments have focused on the modification of the in-medium spin structure.

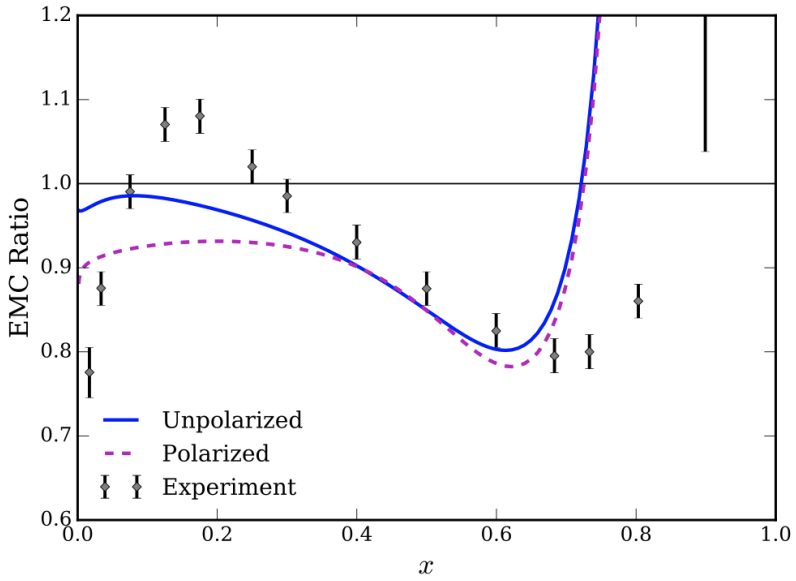

FIG. 1. Unpolarized (blue solid line) and polarized (purple dashed line) mean-field based EMC effect in the QMC model from Ref. [5] (2018). The polarization of the proton is assumed to be 100% for this figure. The results are evolved to Q^2=10 GeV^2. The unpolarized EMC experimental data for nuclear matter is taken from I. Sick and D. Day[10]. A sizeable modification of the polarized structure function is predicted for nuclear matter.

Theoretical work performed since the original proposal was submitted has only underscored the urgency and importance of performing this measurement. In Fig. 1 is shown a recent calculation of the polarized EMC effect predicted in the Quark-Meson Coupling (QMC) model[5], a mean-field approach. The QMC model explicitly allows the quark degrees of freedom to respond self-consistently to the nuclear mean fields, leading to modifications of the internal structure of the bound protons and neutrons; the model neglects short range correlation effects in the nuclear wave functions. In [4] it is argued that short range correlations will cause the participants of the correlation to be depolarized by the interaction, which proceeds through the tensor component of the NN force. From this point of view it is expected that if short range correlations are the sole origin of the unpolarized EMC effect, then a negligible polarized EMC effect will be measured by this experiment, while if the origin of the unpolarized EMC effect is due to the nuclear mean field, the magnitude may be similar to what is shown in the figure or what was found in previous calculations[6], scaled from nuclear matter to ^{7}Li.

In other work published after PAC 42, Ref. [8] used two approaches to describing the unpolarized and polarized EMC effect. The first was to rescale the value of x_{Bj} by a constant factor η. The second is the Modified Sea Scheme (MSS). The x-rescaling approach accounts for the effective mass of the nucleon in the nucleus, while the MSS considers a small virtual pion enhancement in nuclei and models the scaling results by considering the fraction of the nuclear momentum carried by its pionic constituents. Figure 2 shows the effects due to the combination of these two approaches in comparison to previous work by Smith and Miller [11]. For comparison, we also show the prediction by Cloët, Bentz, and Thomas [12, 13]. Because the approach by Fanchiotti *et al.* only modifies x_{Bj}, it is in some sense also a mean-field description of the EMC effect, since it leverages the effects present in all of the nucleons of the medium: binding and the sea.

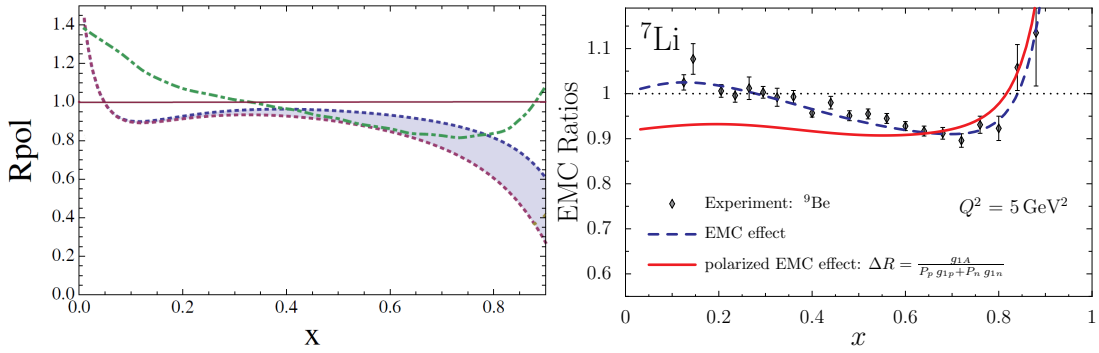

FIG. 2. Left: The polarized EMC ratio band for ^{7}Li as a function of x in the Modified Sea Scheme (MSS) approach (dotted curves) from Ref. [8]. The dot-dashed curve corresponds to the calculation in Ref. [11] with the sea contribution included. The red line at $R_{pol} = 1$ was added as a reference, for clarity. An earlier version of the MSS curve was included in Fig. 5 of the original proposal, prior to its publication in the literature. Right: The prediction from Ref. [12] and Ref. [13].

With the specific choice of Lithium-7 we are taking advantage of the well-established knowledge that the overall spin polarization of the ^{7}Li nucleus concentrates the majority of its polarization on the unpaired $1p_{3/2}$ proton. Detailed modern calculations [14] give the precise value of 86.6% for the degree of polarization of this proton with respect to the overall nuclear polarization. This value is quite consistent with the simpler expectations from shell model calculations. This average proton polarization in ^{7}Li is nearly entirely due to low-momentum (mean-field) protons; in fact, protons with momenta above 300 MeV/c, which are typical of SRC, carry a polarization of less than 5% [14] due to the $^3S_1 \rightarrow {}^3D_1$ tensor coupling that dominates SRCs. Hence, as pointed out in recent publications [4, 6], models that ascribe medium modifications of nucleon structure inside nuclei entirely to SRC would predict no medium modification of the polarized structure function of ^{7}Li compared to a free proton, in stark contrast to predictions based on mean-field models [5].

For this reason, measurement of the spin structure function of ^{7}Li is a uniquely sensitive tool to distinguish between the two leading explanations of the EMC effect: SRC vs. mean field. It is also not excluded to find dramatically larger effects, as were predicted in an approach that is constrained to satisfy the Bjorken Sum Rule[15]. The high polarizability of ^{7}Li, together with novel techniques for the reduction of systematic uncertainties such as a two-cell geometry, allow us to sensitively measure the polarized EMC ratio defined in equation 23 of the original proposal. A much more detailed explanation of the physics goals can be found in the original proposal linked here: https://www.jlab.org/exp_prog/proposals/14/PR12-14-001.pdf.

III. STATUS OF EXPERIMENT PREPARATION

A. CLAS12

CLAS12 has now been in operation for over 2 years for routine data taking and has collected data for four run groups (RG-A, RG-B, RG-K and RG-F). The achievable luminosity and resolution have been demonstrated to be close to the design values and are fully sufficient for the requirements of RG-G.

Run Group G will use CLAS12 in the same configuration as RG-C, with all components of the Forward Detector (FD) and the Central Detector (CD) active. All components of the Forward Tagger (FT) will be removed and the standard Moller shield replaced by the custom "ELMO" shield designed for RG-C, to minimize detector occupancies with rastered beam (see Sections III C and III D). The forward microMEGAS tracker (FMT) will be used to optimize the vertex resolution for forward-scattered particles, for a clean separation between the two target cells. An initial version of the FMT has been used during RG-A but was found to generate high radiative background due to several thick metal components used for its construction. A new version of the FMT has been built by the group at Saclay with much reduced material budget and three (out of a total of 6) layers have been tested successfully during RG-F (Spring 2020). The group at UTFSM is presently analyzing those data to confirm the predicted vertex resolution (from realistic simulations) of 3 mm.

B. Double Cell Polarized Target

Run Group G will utilize the CLAS12 longitudinally polarized target now under construction by a collaboration of the Jefferson Lab Target Group, Old Dominion University, and other universities (CNU, UVa, W&M and UTFSM) which contributed to R&D, simulations, and physics studies[16]. It is anticipated that Run Group C will be the first group of experiments to use the target, most likely in winter-spring 2021-2022. For operation in Run Group G, only two modifications to the target system are required. First, the ammonia target samples for RG-C will be replaced with ^{7}LiD and ^{6}LiH samples. Second, both target samples will be polarized and operated simultaneously during RG-G. Below, we briefly described the current status of the polarized target and discuss the efforts necessary to address both modifications for RG-G.

Nearly all major components for the target system are in-house and tested, either in final or prototype form. This includes all electronics, microwave generator and wave guide components, as well as the 1 K refrigerator and pumps. The CLAS12 solenoid will provide the 5 T field for polarizing the target samples in the longitudinal direction [17]. The samples will be cooled to 1 K using a custom-built, high cooling power ^{4}He evaporation refrigerator currently undergoing tests in the Target Group's lab [18]. Three cool-downs have been performed to date, each highly successful. These have demonstrated a base temperature below 1 K, a cooling power of 1 W at 1.08 K, and a daily consumption of liquid helium under 50 liters. Based on previous experience at JLab, the refrigerator features a number of innovative design elements that are intended to make it more reliable and more easily serviced, and to reduce the overhead of its operation. Target polarization will be measured using new NMR Q-meters designed and constructed by the JLab Target Group and the JLab Fast Electronics Group [19]. Prototypes of the new system have demonstrated equal or superior performance compared to the industry-standard Liverpool Q-meter [20], which is no longer in production and has become difficult to maintain due to its reliance on obsolete components. A new target insertion cart for the Hall B rail system is now under construction that will permit precise alignment of the system on the Hall B beam line. Furthermore, all essential electronic, vacuum, and piping components for the target will be mounted directly on the cart, reducing the time needed to install the system in the hall. Design is also underway of beam-ready replacements for certain prototype components of the refrigerator, such as the retractable helium bath and the thin, downstream portion of the vacuum chamber. In particular, a "trolley" system has been designed and tested that allows the rapid exchange of target samples without having to open the beam line up. This system will allows us pre-fill complete target samples of various compositions (including ammonia and other auxiliary targets for calibration) and exchange them frequently. This will be useful for minimizing systematic (acceptance) uncertainties by allowing us to swap the position of the ^{7}LiD and ^{6}LiH samples. All parts not already on hand will be built in the near future, and the target system can be available for installation in Hall B in summer 2021.

In ^{6}LiD deuteron (^{6}Li) polarizations of 32% (31%) have been achieved at 1 K and 5 T. Even higher polarizations, exceeding 90% (80%), have been observed for protons (^{7}Li) in ^{7}LiH. For optimum results, the target sample should be irradiated to a flux of about 3.7×10^{17} e$^-$ cm^{-2} in a narrow temperature band around 183 K [21]. This will be performed using the 10 MeV electron beam of JLab's new Upgraded Injector Test Facility and a custom-built, variable temperature cryostat.

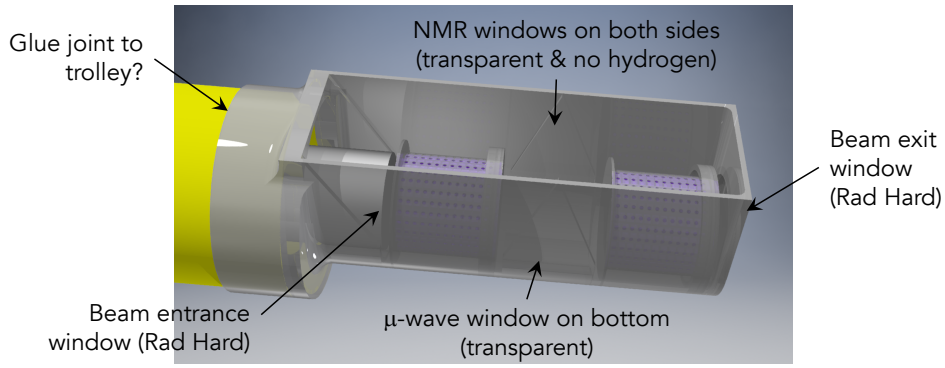

FIG. 3. Design of a double-cell target nosecone.

Dynamic nuclear polarization is typically performed at a fixed magnetic field setting, say 5 T, and irradiating the sample with RF that is slightly off-center from the corresponding electron spin resonance frequency $\nu_e \simeq 140$ GHz. Positive or negative nuclear polarizations can be generated by adjusting the RF frequency below or above ν_e by approximately the NMR frequency ν_n. Alternatively, one may fix the RF at the ESR frequency and adjust the magnetic field by the appropriate amount (about $\pm$ 50 G at 140 GHz). We will use this latter method to simultaneously

polarize two target samples in opposite directions or of different species (e.g., deuteron vs. hydrogen), as required for RG-G; see Fig. 3. The local field around each sample will be shifted from the 5 T central field using modest superconducting coils fitted inside the 1 K refrigerator. The design of the coils will be guided by an algorithm that adjusts the position, number of windings, and current for each coil to achieve the desired field value at each sample [22]. The measured field map for the CLAS12 solenoid is included in the simulation.

To test the success of the algorithm and to demonstrate the double-cell polarization technique, tests have been conducted using prototype coils of normally-conducting copper and samples of two-part epoxy doped with the nitroxyl radical TEMPO. For convenience, the tests were performed at 77 K using a warm-bore 5 T solenoid. Four coils of 32 AWG copper wire were wound onto an aluminum carrier (Fig. 4), with the location, widths, and number of layers determined by precision grooves machined into the carrier. The coils were fixed to the carrier using GE 7031 varnish.

Coil	**z (cm)**	**# of Windings**	**Current (A)**
1	-3.5	132	0.940
2	-0.6	171	3.305
3	0.6	172	-3.284
4	3.5	131	-0.929

TABLE I. Parameters of prototype coil set. For each coil, the inner radius is 2.7 cm with windings distributed between four layers.

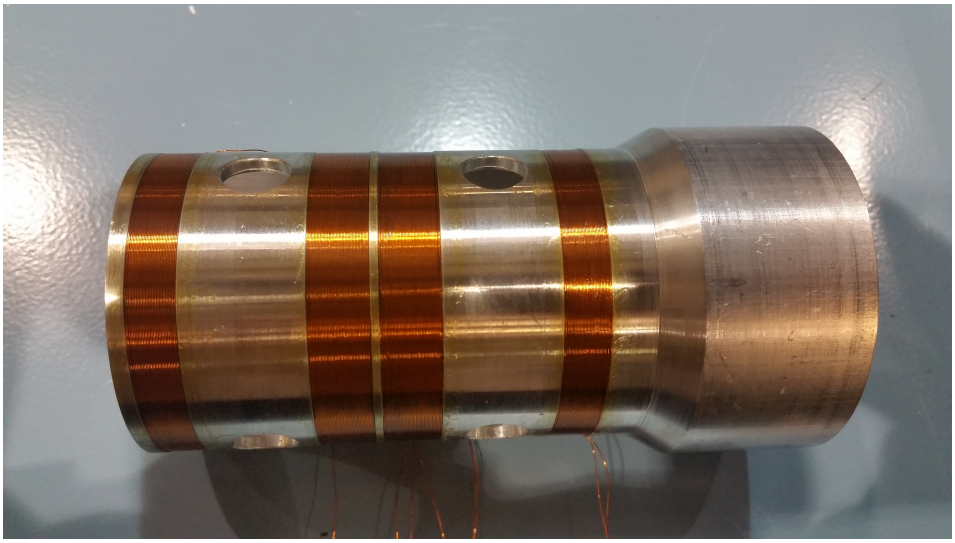

FIG. 4. Shim coils on aluminum carrier.

The results, shown in Fig. 5, clearly demonstrate the efficacy of both the algorithm and the double-polarization technique. Two NMR peaks of opposite polarization could be obtained using a single NMR coil that encompassed both samples. The microwave frequency was fixed approximately halfway between the normal frequencies for positive and negative polarizations.

C. Beam Raster

To maintain high polarization, the ionizing radiation dose to the target must be evenly distributed to its entire volume by rastering the electron beam over the sample's 1 cm radius. This is accomplished using two upstream sets of x-y dipole magnets synchronously driven by high-current, dipolar power supplies. The electron beam is deflected by the first set of magnets and then made parallel to the beam line by the second set. One power supply feeds both x magnets, arranged such that the magnetic fields are 180° out of phase; the y magnets operate in a similar fashion using a second power supply. RGC will be the first experiments to utilize a rastered beam in Hall B since the 12 GeV energy upgrade.

It has been determined that the existing raster magnets from the 6 GeV program in Hall B are adequate for the RG-C and RG-G experiments, and appropriate locations on the beam line have been specified. A new spiral raster

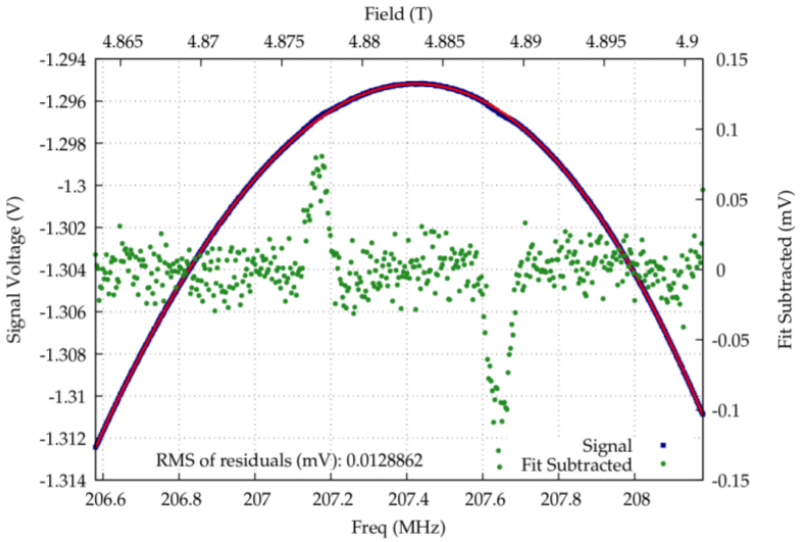

FIG. 5. NMR signal showing opposing polarizations in two adjacent cells held in two shim field regions, driven by a single microwave frequency.

control module for the power supplies has been designed, constructed, and tested by the JLab Fast Electronics Group, and ±240 A power supplies from Danfysik are on hand. Together, they will raster the electron beam in a spiral pattern at constant linear speed, thus giving a uniform illumination over the face of the target sample. The period of a full spiral-in, spiral-out cycle will be about 1 s.

D. New Moller Shield and Drift Chamber Occupancies

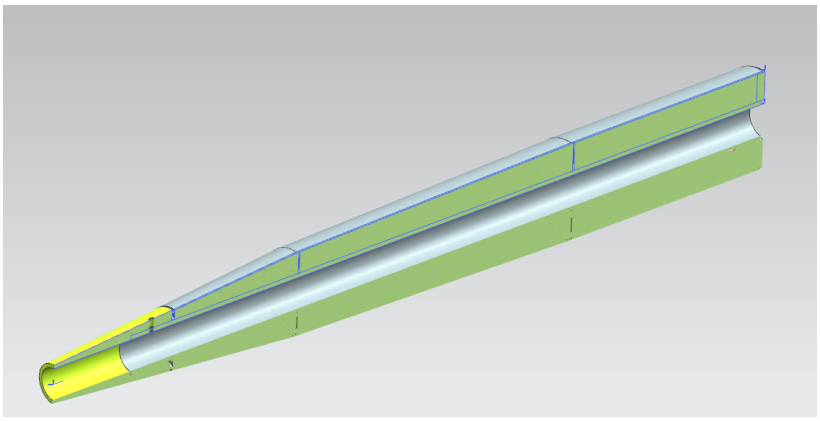

FIG. 6. Engineering drawing of the new Moller shield "ELMO".

As part of the preparations for RG-C, we have designed a new Moller shield for use with rastered beam on a polarized target. The design is shown in Fig. 6 and has been validated by the Hall-B engineer, R. Miller. It is a modified version of the "FTOff" Moller shield which has been used during previous run groups (including RG-A and RG-F), and it has been optimized to contain the electromagnetic background produced by the electron beam as far as 1 cm off the nominal beam axis (to accommodate rastering). RG-G (as well as the first installment of RG-C) will use a configuration with the Forward Tagger (FT) removed and this new Moller shield installed, to be able to run with the highest luminosity possible (as originally proposed). The FT would require a much smaller raster radius and significantly lower luminosity, and is not needed for the physics goals of this experiment.

The expected suppression of background in the drift chambers is shown in Fig. 7 for the case of the RG-C "APOLLO" target. As can be seen, the Region I DC occupancy will be reduced by a factor 2 and will be similar to that observed

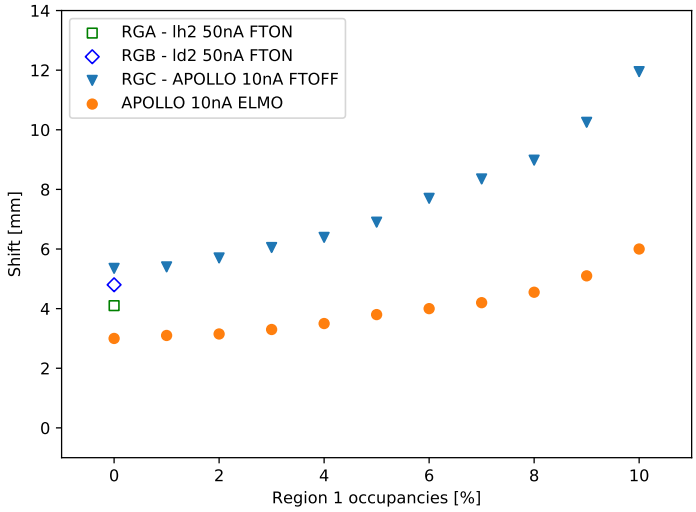

FIG. 7. GEMC simulation of DC occupancies vs. raster size. The empty square and diamond points at 0 mm shift correspond to the observed DC occupancies for RGA and RGB groups in the FTon configuration, the filled triangles are for the APOLLO target with the FTOff shielding and the filled circles are for APOLLO with the ELMO shield. RG-G will use the ELMO Moller shield.

during actual RG-A running conditions. The double-cell target to be used in RG-G is very similar in overall design, total target thickness and expected luminosity as "APOLLO" and hence should have similarly acceptable backgrounds.

IV. SUMMARY

Since RG-G has been approved, the community's interest to measure the EMC effect in polarized structure functions has only grown and the physics case remains compelling. No comparable data have been collected anywhere or are likely to be available in the foreseeable future. Measuring the polarized EMC effect remains a crucial centerpiece for a complete understanding of the modification of nucleon structure functions in nuclei, which is a central component of the Physics program at Jefferson Lab in the 12 GeV era.

The collaboration and Jefferson Lab have made a major investment in the equipment needed for RG-G, including substantial support by an NSF MRI awarded to a consortium of universities (CNU, ODU, and UVa) and a significant development effort at UTFSM (Chile). Members of the collaboration have invested significant time and effort into all aspects of the preparation of this experiment - from prototyping and building the double-celled polarized target to simulations and design of all necessary beam line equipment. The experiment will be ready to run anytime after the conclusion of Run Group C (tentatively scheduled for 2022). We request that the PAC reaffirm the original approval of this run group.

REFERENCES

[1] S. Kuhn, W.K. Brooks, et al. The EMC Effect in Spin Structure Functions. http://www.jlab.org/exp_prog/proposals/14/PR12-14-001.pdf.

[2] B. Schmookler, M. Duer, A. Schmidt, S. Gilad, L.B. Weinstein, E. Piasetzky, and O. Hen. Isospin Dependence of the EMC effect and Short range Correlations. *arXiv*, 1711.00960, 11 2017.

[3] B. Schmookler et al. Modified structure of protons and neutrons in correlated pairs. *Nature*, 566(7744):354–358, 2019. https://dx.doi.org/10.1038/s41586-019-0925-9.

[4] Anthony W. Thomas. Reflections on the Origin of the EMC Effect. *Int. J. Mod. Phys. E*, 27(12):1840001, 2019.

[5] S. Tronchin, H.H. Matevosyan, and A.W. Thomas. Polarized EMC effect in the QMC model. *Phys. Lett. B*, 783:247–252, 2018. https://doi.org/10.1016/j.physletb.2018.06.065, https://arxiv.org/abs/1806.00481.

[6] I C Cloët, R Dupré, S Riordan, W Armstrong, J Arrington, W Cosyn, N Fomin, A Freese, S Fucini, D Gaskell, C E Keppel, G A Miller, E Pace, S Platchkov, P E Reimer, S Scopetta, A W Thomas, and P Zurita. Exposing novel quark and gluon effects in nuclei. *Journal of Physics G: Nuclear and Particle Physics*, 46(9):093001, jul 2019. https://doi.org/10.1088/1361-6471/ab2731.

[7] X.G. Wang, A.W. Thomas, and W. Melnitchouk. Do short-range correlations cause the nuclear EMC effect in the deuteron? *arXiv*, 2004.03789, 4 2020. https://arxiv.org/abs/2004.03789.

[8] Huner Fanchiotti, Carlos A. García Canal, Tatiana Tarutina, and Vicente Vento. Medium effects in DIS from polarized nuclear targets. *The European Physical Journal A*, 50(7), Jul 2014. https://doi.org/10.1140/epja/i2014-14116-8, https://arxiv.org/abs/1404.3047.

[9] L.B. Weinstein, E. Piasetzky, D.W. Higinbotham, J. Gomez, O. Hen, and R. Shneor. Short Range Correlations and the EMC Effect. *Phys. Rev. Lett.*, 106:052301, 2011.

[10] Ingo Sick and Donal Day. The EMC effect of nuclear matter. *Physics Letters B*, 274(1):16 – 20, 1992.

[11] Jason Robert Smith and Gerald A. Miller. Polarized quark distributions in nuclear matter. *Phys. Rev. C*, 72:022203, 2005.

[12] I.C. Cloet, Wolfgang Bentz, and Anthony William Thomas. Spin-dependent structure functions in nuclear matter and the polarized EMC effect. *Phys. Rev. Lett.*, 95:052302, 2005.

[13] I.C. Cloet, Wolfgang Bentz, and Anthony William Thomas. EMC and polarized EMC effects in nuclei. *Phys. Lett. B*, 642:210–217, 2006.

[14] R. B. Wiringa, R. Schiavilla, Steven C. Pieper, and J. Carlson. Nucleon and nucleon-pair momentum distributions in $A \leq 12$ nuclei. *Phys. Rev. C*, 89:024305, Feb 2014.

[15] V. Guzey and M. Strikman. Nuclear effects ing1a(x,q2)at smallxin deep inelastic scattering on7liand3he. *Physical Review C*, 61(1), Dec 1999.

[16] D.M. Aliaga, P. Bunout, V. Arredondo, W.K. Brooks, R. Feick, R. Gers, H. Hakobyan, C.P. Romero, and K. Slifer. A new method for fabrication of cryo-solids for polarized targets. *Nuclear Instruments and Methods in Physics Research Section A: Accelerators, Spectrometers, Detectors and Associated Equipment*, 972:164061, 2020. https://doi.org/10.1016/j.nima.2020.164061.

[17] R. Fair *et al.* The CLAS12 Superconducting Magnets. *Nuclear Instruments and Methods in Physics Research Section A: Accelerators, Spectrometers, Detectors and Associated Equipment*, 962:163578, 2020.

[18] J. Brock. 1 K Refrigerator for the CLAS12 Polarized Target. In *Proceedings of the 18th International Workshop on Polarized Sources, Targets, and Polarimetry (PSTP 2019)*, to be published.

[19] J. Maxwell. "NMR Polarization Measurements for Jefferson Lab's Solid Polarized Targets". In *Proceedings of the 17th International Workshop on Polarized Sources, Targets, and Polarimetry (PSTP 2017)*, 2017.

[20] G.R. Court, D.W. Gifford, P. Harrison, W.G. Heyes, and M.A. Houlden. A High Precision Q-meter for the Measurement of Proton Polarization in Polarised Targets. *Nuclear Instruments and Methods in Physics Research Section A: Accelerators, Spectrometers, Detectors and Associated Equipment*, 324(3):433 – 440, 1993.

[21] S. Bueltmann et al. A study of lithium deuteride as material for a polarized target. *Nuclear Instruments and Methods in Physics Research Section A: Accelerators, Spectrometers, Detectors and Associated Equipment*, 425:23, 1999.

[22] V. Lagerquist. Magnetic Field Requirements for the CLAS12 Polarized Target. In *Proceedings of the 18th International Workshop on Polarized Sources, Targets, and Polarimetry (PSTP 2019)*, to be published.